PHYS 243 Final Paper: Topological Phenomena and Quantum Computing in Rydberg Systems

Andrew Pocklington

March 24, 2020

1 Introduction

1.1 Why Topological Qubits

The idea of quantum computation is usually attributed to Feynman [1], who proposed the concept in 1982. Nearly 40 years later, though, the world's most advanced quantum computer still uses only 53 qubits [2]. One important reason that seemingly so little progress has occurred in the last 4 decades is that quantum systems are incredibly sensitive to their environment. A traditional qubit is a physical two level quantum system, in which one level represents 0, and the other level represents 1. The physical construction of these systems has proved to be a difficult task, though, as there are a few fundamental criteria these systems need to meet in order to serve well as quantum computing platforms. The first is long coherence times, where long is relative to the time needed to implement gates; this is necessary for the obvious reason that if the system decoheres before gates can be implemented, no useful computations can be performed. The second is high gate fidelity; algorithm's rely on the fact that gates do what they are supposed to, and even error correcting codes need gates to reach at least a certain threshold fidelity in order to work [3]. Finally, while these first two criteria give a functional quantum computer, to get a *useful* one, we require scalability. To do more interesting physics and simulations, the ability to create larger computers with more qubits will be essential.

Quantum Computer Architecture Comparison

System	Coherence Time	1 Qubit Gate Fidelity	2 Qubit Gate Fidelity
Superconductor	140 μs [4]	99.85% [2]	99.35% [2]
Trapped Ion	600 s [5]	99.99% [5]	99.9% [5]
Neutral Atom	47μs [6]	99% [6]	97.3% [6]
Quantum Dot	40 ms [7]	99.9% [7]	90% [7]
NV Center	0.6 s [7]	99.95% [7]	96% [7]

Numerous systems have been proposed, each with their own successes and drawbacks with regard to coherence, fidelity, and scalability, see the table above. From a quick glance,

a fidelity of over 99% appears to be quite good; unfortunately, though, errors quickly add up. Even Google's landmark paper, which used only 53 qubits and about 20 gates, had a success rate of less than a percent [2]. However, an exciting platform that has *not* yet been realized is a topological qubit, which relies on a topological property of the system in order to store quantum information. These systems, originally proposed by Kitaev, [8], are inherently robust to noise, meaning that they can achieve theoretically unbounded gate fidelities and coherence times. It is for this reason that topological qubits could be a huge leap froward in quantum computing architecture.

1.2 What Are Topological Qubits

Mathematically, a topological property of a system is something that is invariant under local homeomorphisms [9], which is a continuous deformation. Thinking of environmental noise as local fluctuations in the system, this is exactly the kind of property desired in quantum computing architecture. Thus, if we can isolate properties that are immune to noise and background fluctuations, it would dramatically improve the ability to store quantum information. There are many ways to introduce topological invariants into a system; this paper will examine braiding in non-abelian anyons.

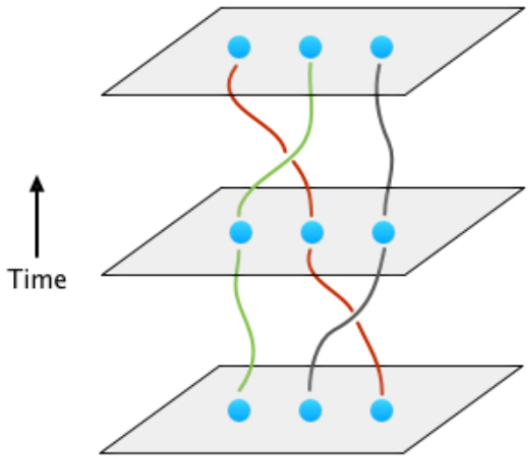

Figure 1: This image shows the topology of the world lines of braided particles. Note that the world lines can move around continuously, but as long as they don't cross, the braid pattern is preserved. Thus, this is a topological invariant, and very robust.

One of the most important principles in quantum mechanics are the exchange statistics of different types of particles. Classically, swapping two identical particles does not change the system, but in quantum mechanics, this does not always hold. The two fundamental types of particles are bosons, which behave classically under exchange, and fermions, which pick up a phase of -1 under exchange. However, there are more exotic types of particles, *any*ons, which can pick up *any* phase under exchange. A useful way to express these relations is in terms of particle creation and annihilation operators. Similarly to the way the creation and annihilation operators added or removed a quanta of energy in a harmonic oscillator, particle operators add or remove a particle from the vacuum state. Thus, if we have some type of particle a, we can think of two operators $a^\dagger(\vec{\mathbf{x}}), a(\vec{\mathbf{x}})$ which add and remove an a particle at position $\vec{\mathbf{x}}$, respectively. For the remainder of this paper, we will be working on a lattice, so position can just be indexed by a lattice site, i.e. $a(\vec{\mathbf{x}}) \to a_i$ for some $i \in \mathbb{N}$. Using this notation, the commutation relations for an anyon is

$$a_i a_j^\dagger = e^{i\phi} a_j^\dagger a_i \tag{1}$$

where $\phi \in [0, 2\pi)$. What makes these particles so interesting is that upon swapping them twice, so that they end up in their original locations, the wavefunction describing them need not return to itself. The particles have been braided around each other, and there is a quantum memory that remembers where they have been. The topology of the world lines of the particles, then, contains information which is incredibly robust to noise, see fig. 1. In order to lose this information and decohere, the particles would have to physically move around each other.

However, particle statistics can behave even more strangely. A number of models [10] have been shown to exhibit non-abelian statistics, which means that the order in which swaps are performed matters. When this occurs, exchange operators form a non-abelian group, called the braid group. An example of this are the Majorana fermions which form at boundary defects of the Kitaev chain model [10, 11] (discussed more later). If γ^1, γ^2 are two Majorana creation/annihilation operators (note that a Majorana fermion is defined such that $\gamma^\dagger = \gamma$, so the creation operator is the same as the annihilation operator), then under a clockwise exchange,

$$\gamma^1 \to -\gamma^2 \tag{2}$$
$$\gamma^2 \to \gamma^1 \tag{3}$$

but under a counterclockwise exchange

$$\gamma^1 \to \gamma^2 \tag{4}$$
$$\gamma^2 \to -\gamma^1 \tag{5}$$

In general, we will define U_{ij} to exchange the i^{th} and j^{th} particles. As long as there are at least 3 of them, the braid group generated by the U_{ij}'s forms a non-abelian subgroup of $U(2)^{\otimes n}$, where n is the total number of Majoranas in the system.

Finally, non-abelian anyons have one more important quality, which is their fusion rules. This is the process in which two anyons fuse together to form a new anyon. An example of this are Fibonacci anyons, which come in 2 flavors, the trivial $\mathbf{1}$, and the τ. If we let $\times$ denote the fusion of two Fibonacci anyons, then we can write down their fusion rules as [12]:

$$\tau \times \mathbf{1} \to \tau \tag{6}$$
$$\mathbf{1} \times \tau \to \tau \tag{7}$$
$$\tau \times \tau \to \mathbf{1} \oplus \tau \tag{8}$$
$$\mathbf{1} \times \mathbf{1} \to \mathbf{1} \tag{9}$$

where $\oplus$ denotes a superposition of both. Again, the topology of the world lines of the particles and how they fuse together is inherently protected from noise and decoherence in the system.

Having established some motivation for what topological qubits are, and why they are interesting, we will now briefly explore the neutral atom platform, so as to gain some insight into how they can be simulated in a real, physical system.

2 Rydberg Systems

Neutral atoms provide a novel system for quantum simulation, and therefore may be able to realize some topological phenomena that have so far remained elusive in experiments. Here, a brief overview of the ingredients of a Rydberg system on neutral atoms will be provided.

Rydberg states are simply atomic states with a large principal quantum number, n. Usually, Alkali atoms are used to construct these states, since they are Hydrogen like, and have only a single valence electron. The simplicity of this structure allows much carry over from the study of the Hydrogen atom [13]. (Alkaline earth metals, with two valence electrons, are also used, although this approach is slightly less common [14].) A few interesting characteristics develop when atoms are excited to large n values. Notably, the extent of the wavefunction grows proportionally to n^2, so while a ground state atom may be on the order of 1Å, for example the $80S$ state of rubidium 87 is 500nm. This in turn causes a massive increase in the interactions between different atoms, with the Van-Der-Waals C_6 coefficient growing like n^{11} [13]. What this means is that they can be well separated spatially while still achieving large interactions. Because energy is proportional to frequency, and hence inversely proportional to time, one can thus achieve fast gates, which is crucial for quantum computation and simulation. This goes hand in hand with the other important characteristic of Rydberg states, which is that the lifetime scales like n^3 [13]. This means that while the radiative lifetime of the D2 line of Rubidium 87 is 27ns [15], the lifetime of the $80S$ state is 200μs [13]. Long lifetimes are also critical to being able to perform the necessary gates before the system decoheres.

The next important point to note in neutral atom systems is the control and scalability. Neutral atoms can be easily held in optical tweezers [6], which use the Stark shift to create a potential well for the atom. This is a phenomena in which the energy levels of a dipole are shifted when in the presence of a strong, far detuned light field:

$$\Delta E = \frac{\hbar \Gamma^2 I}{8 \delta I_{sat}} \tag{10}$$

where Γ is the radiative lifetime, δ is the detuning of the laser, and I_{sat} the saturation intensity of the transition. Optical tweezers work in the regime of red-detuning far from any transition, which makes the energy change negative, and proportional to the intensity of the light. Thus, by making a very tightly focused laser beam, in which the intensity has a very large gradient at the focal point, the atom sees a spatial potential well. In this way, atoms can be trapped in the focus of the laser. Further, through a process called light-assisted collisions [16], any time two atoms enter a tweezer at the same time, they are both immediately expelled. This means that each tweezer holds exactly one atom or zero atoms. Hence, this platform allows single site resolution, control of each qubit, and the ability to conduct single site readout of the entire ensemble of tweezers through a single image.

A phenomena critical to much of the rich Rydberg physics is the blockade regime. Because of the enormous Van-Der-Waals interactions experienced by neighboring Rydberg states, when they are brought near each other, they experience a shift in their energy levels. In this way, laser light that may have previously been on resonance with a transition no longer is,

and hence two atoms sitting next to each other cannot both be excited to a Rydberg state simultaneously. When this occurs, we would say they have been blockaded.

Say two atoms are brought close together, both in the ground state $|g\rangle$. If one then applies a laser field resonant with a transition to a Rydberg state, $|r\rangle$, both atoms will want to undergo Rabi oscillations into this excited state. However, because of this blockade mechanism, only one can be in $|r\rangle$ at any given time, and so instead $|gg\rangle \rightarrow \frac{1}{\sqrt{2}}(|rg\rangle + |gr\rangle)$ [17], see fig. 2.

From this, one can engineer a Hamiltonian out of Rydberg interactions. The blockade mechanism gives [18]

$$H = \sum_{i \neq j} \frac{C_6}{|\mathbf{r_i} - \mathbf{r_j}|^6} n_i n_j \tag{11}$$

where n_i is the number of Rydberg excitation at site i, either 0 or 1, and C_6 is the Van-Der-Waals coefficient. By assembling the atoms into a chain, and separating them such that only nearest neighbors feel an appreciable blockade, this becomes

$$H = J \sum_{i=1}^{N-1} n_i n_{i+1} \tag{12}$$

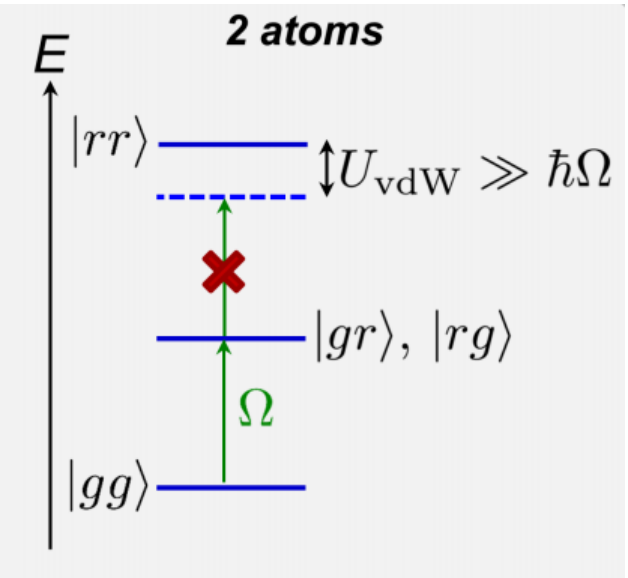

Figure 2: Blockade regime for Rydberg atoms. Two atoms placed close to each other cause the Rydberg level to be shifted up by the Van-Der-Waals interaction, meaning they cannot both be simultaneously excited by the same light field. Image from [13].

where J is a constant which depends on the specific Rydberg state and the lattice spacing, and the chain is N atoms long. Another term comes from the driving field, which appears as [6]

$$H = \sum_{i=1}^{N} \frac{\Omega}{2} \sigma_i^x - \Delta n_i \tag{13}$$

where Ω is the Rabi frequency induced by the laser source, and Δ is the detuning from resonance on the transition. It is interesting to note that these terms exactly define the transverse field Ising model.

A final interesting interaction that can occur is when a microwave field couples two different Rydberg states together, which drives coherent oscillations between two different Rydberg states, where now $|0\rangle$ and $|1\rangle$ are both excited states, instead of an excited state and a ground state. This gives the interaction [19]

$$H = \frac{1}{2} \sum_{i \neq j} \frac{C}{|\mathbf{r_i} - \mathbf{r_j}|^3} (\sigma_i^+ \sigma_j^- + \sigma_j^+ \sigma_i^-) \tag{14}$$

Note this is only cubicly surpressed in distance because it is a dipole-dipole coupling of the Rydberg states, not a Van-Der-Waals interaction. Again, by properly tuning the lattice spacing, this can be converted into

$$H = \frac{J}{2}\sum_{i=1}^{N-1}(\sigma_i^+\sigma_{i+1}^- + \sigma_{i+1}^+\sigma_i^-) \tag{15}$$

This is the last element needed to begin constructing interesting topological properties.

3 Example Models

Now, using the tools of Rydberg systems, we will construct possible models that exhibit emergent topological phenomena, and discuss how they might be able to function as topological qubits.

3.1 Kitaev Chain

The Kitaev Chain is incredibly rich in topology. Both the qubits and their gates would experience topological protection, which would extend both coherence time and fidelity into unprecedented regimes if it were possible to implement. This was originally proposed as a system for spinless fermions, which exhibited topologically protected Majorana zero modes. Initially, this seems to be a cause for concern, since if one treats a Rydberg excitation as a quasi-particle on a lattice, it is not a spinless fermion, but instead a hardcore boson. This is because it obeys bosonic exchange statistics, and is also limited to a single excitation per lattice site (making it "hardcore"). Luckily, the Jordan-Wigner transformation [20] is a mapping from hardcore bosons to spinless fermions and vice-versa. We will let $b_i, b_i^\dagger$ be our bosonic operators, defined by the canonical commutation relations

$$[b_i, b_j] = [b_i^\dagger, b_j^\dagger] = 0 \tag{16}$$

$$[b_i, b_j^\dagger] = \delta_{ij}\sigma_i^z \tag{17}$$

$$\{b_i, b_j^\dagger\} = \mathbf{1} \tag{18}$$

$$(b_i)^2 = (b_i^\dagger)^2 = 0 \tag{19}$$

where the last equation is the condition of being hardcore. If we now define

$$c_i = \left(\prod_{k=1}^{i-1}\sigma_k^z\right) b_i \tag{20}$$

$$c_i^\dagger = \left(\prod_{k=1}^{i-1}\sigma_k^z\right) b_i^\dagger \tag{21}$$

it can be readily checked that $c_i, c_i^\dagger$ obey the commutation relations of fermions. Now, the Hamiltonian defined by Kitaev is [11]

$$H = \sum_{i=1}^{N-1} tc_{i+1}^\dagger c_i + \Delta c_{i+1}^\dagger c_i^\dagger + \text{h.c.} \tag{22}$$

This is a model of a wire sitting on top of a superconductor, where $c_{i+1}^\dagger c_i + c_i^\dagger c_{i+1}$ represents electrons moving along the wire, and $c_{i+1}^\dagger c_i^\dagger + c_i c_{i+1}$ is a Cooper pair tunneling onto and off of the wire from the superconductor below. Using the Rydberg dipole-dipole interaction as defined before, written in terms of the quasi-particle operators instead of the Pauli operators, we might create the Hamiltonian:

$$H = \sum_{i=1}^{N-1} t b_{i+1}^\dagger b_i + \Delta b_{i+1}^\dagger b_i^\dagger + \text{h.c.} \tag{23}$$

which looks like Kitaev's model, but has the bosonic operators instead of the fermionic ones. Luckily, if we use the Jordan-Wigner transformation to map this onto a fermionic Hamiltonian, we arrive at

$$\begin{aligned} H &= -t c_i^\dagger c_{i+1} - \Delta c_i c_{i+1} + h.c. && (24)\\ &= -t \pi_1^{i-1} b_i^\dagger \pi_1^i b_{i+1} - \Delta \pi_1^{i-1} b_i \pi_1^i b_{i+1} + h.c. && (25)\\ &= -t b_i^\dagger \sigma_i^z b_{i+1} - \Delta b_i \sigma_i^z b_{i+1} + h.c. && (26)\\ &= -t b_i^\dagger b_{i+1} + \Delta b_i b_{i+1} + h.c. && (27) \end{aligned}$$

where we have abbreviated $\prod_{k=1}^{i} \sigma_k^z$ as π_1^i. Thus, the spinless fermion model maps directly onto a bosonic Ising chain [21], which is a readily available tool to the Rydberg platform [22]. Following Kitaev's original analysis, the next step is for us to define Majorana operators, which have the special property of being self-adjoint. Let us define two types of Majorana at each lattice site:

$$\gamma_i^1 = \frac{1}{\sqrt{2}}(c_i + c_i^\dagger) \tag{28}$$

$$\gamma_i^2 = \frac{1}{\sqrt{2}i}(c_i - c_i^\dagger) \tag{29}$$

By inspection, these operators obey $(\gamma_i^j)^\dagger = \gamma_i^j$. Further, inverting these equations,

$$c_i = \frac{1}{\sqrt{2}}(\gamma_i^1 + i\gamma_i^2) \tag{30}$$

$$c_i^\dagger = \frac{1}{\sqrt{2}}(\gamma_i^1 - i\gamma_i^2) \tag{31}$$

From the inversion, it becomes clear that each γ_i^j represent neither a particle nor a hole, but instead a superposition of the two. To make an actual particle, a sum of 2 Majoranas is

necessary. The last thing to check are the anticommutation relations of γ.

$$\begin{aligned}
\{\gamma_i^1, \gamma_j^1\} &= \frac{1}{2}((c_i + c_i^\dagger)(c_j + c_j^\dagger) + i \leftrightarrow j) \\
&= \frac{1}{2}(\{c_i, c_j\} + \{c_i, c_j^\dagger\} + \{c_i^\dagger, c_j\} + \{c_i^\dagger, c_j^\dagger\}) \\
&= \frac{1}{2}(0 + \delta_{ij} + \delta_{ij} + 0) \\
&= \delta_{ij} \qquad (32) \\
\{\gamma_i^1, \gamma_j^2\} &= \frac{1}{2i}((c_i + c_i^\dagger)(c_j - c_j^\dagger) + (c_j - c_j^\dagger)(c_i + c_i^\dagger)) \\
&= \frac{1}{2i}(\{c_i, c_j\} - \{c_i, c_j^\dagger\} + \{c_i^\dagger, c_j\} - \{c_i^\dagger, c_j^\dagger\}) \\
&= \frac{1}{2i}(0 - \delta_{ij} + \delta_{ij} - 0) \\
&= 0 \qquad (33) \\
\{\gamma_i^2, \gamma_j^2\} &= \frac{-1}{2}((c_i - c_i^\dagger)(c_j - c_j^\dagger) + i \leftrightarrow j) \\
&= \frac{-1}{2}(\{c_i, c_j\} - \{c_i^\dagger, c_j\} - \{c_i, c_j^\dagger\} + \{c_i^\dagger, c_j^\dagger\}) \\
&= \frac{-1}{2}(0 - \delta_{ij} - \delta_{ij} + 0) \\
&= \delta_{ij} \qquad (34) \\
(\gamma_i^1)^2 &= (\gamma_i^2)^2 = 1 \qquad (35)
\end{aligned}$$

Using $\{\gamma_i^1, \gamma_j^2\} = \{\gamma_j^2, \gamma_i^1\} = \{\gamma_i^2, \gamma_j^1\}$ under a trivial redefinition $i \leftrightarrow j$, we get $\{\gamma_i^2, \gamma_j^1\} = 0$. Thus,

$$\{\gamma_i^\alpha, \gamma_j^\beta\} = \delta_{ij}\delta_{\alpha\beta} \qquad (36)$$

Now, we will see how these new operators transform our Hamiltonian. For simplicity, we will stop including the sum, and i will be implicitly summed over unless otherwise specified. Letting $\Delta = t$,

$$\begin{aligned}
H' &= -t(c_i c_{i+1} + c_i^\dagger c_{i+1} + h.c.) \\
&= \frac{-t}{2}((\gamma_i^1 + i\gamma_i^2)(\gamma_{i+1}^1 + i\gamma_{i+1}^2) + (\gamma_i^1 - i\gamma_i^2)(\gamma_{i+1}^1 + i\gamma_{i+1}^2) + h.c.) \\
&= -2it\gamma_i^1\gamma_{i+1}^2 \qquad (37)
\end{aligned}$$

We have already arrived at a rather significant result from this analysis in that γ_1^2 and γ_N^1 do not appear in the Hamiltonian, and therefore have no energy cost in the system. We can construct a new fermionic operator

$$f = \frac{1}{\sqrt{2}}(i\gamma_1^2 + \gamma_N^1) \qquad (38)$$

which creates a highly nonlocal "Majorana Zero Mode", so named because it is made of 2 Majorana edge modes and adds no energy to the system.

Thus, when this operator acts on the ground state, it produces a second, orthogonal and degenerate ground state for the system. One more simplification reduces the Hamiltonian even further, allowing us to easily read off the states. Take

$$d_i = \frac{1}{\sqrt{2}}(i\gamma_i^1 + \gamma_{i+1}^2) \tag{39}$$

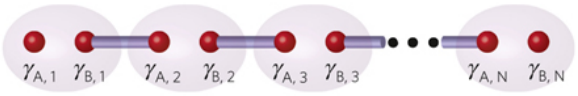

Figure 3: This graphic shows how the d_i operators pair neighboring Majorana's, leaving the ends out of the Hamiltonian, and thus protected. Image from [10].

Note that the d operator relates Majoranas from different physical lattice sites. In effect, it couples "half" an electron with each of its neighbors, importantly preserving the fact that on each end, one "half" will remain uncoupled. Our d quasi-particle number operator is:

$$d_i^\dagger d_i = \frac{1}{2}(\gamma_i^1\gamma_i^1 - i\gamma_i^1\gamma_{i+1}^2 + i\gamma_{i+1}^2\gamma_i^1 + \gamma_{i+1}^2\gamma_{i+1}^2) = 1 - i\gamma_i^1\gamma_{i+1}^2 \tag{40}$$

where we use the fact that $(\gamma_i^j)^2 = 1$ and anticommutation to arrive at the final identity. It now becomes clear that our Hamiltonian can be written as

$$H = 2t(d_i^\dagger d_i - 1) \tag{41}$$

Where the ground state obeys $d_i|\psi_{gs}\rangle = 0\ \forall i$. Because these end modes do not appear in the Hamiltonian, they remain topologically protected from perturbations in the Hamiltonian [10, 11]. They will always appear at boundary defects of the chain. Further, they display the braiding statistics discussed in the previous section [10]. A physical qubit can be realized as the two degenerate ground states of the chain, i.e.

$$|0\rangle = |\psi_{gs}\rangle \tag{42}$$
$$|1\rangle = f^\dagger|0\rangle \tag{43}$$

From this point forward, to simplify notation, we will drop the upper and lower indices, and just label a collection of Majoranas as γ_i. Recall that the braid statistics of the Majoranas are defined as

$$\gamma_1 \to \pm\gamma_2 \tag{44}$$
$$\gamma_2 \to \mp\gamma_1 \tag{45}$$

where the sign depends on the direction of rotation. If we let $U_{12}^\pm = 1/\sqrt{2}(1 \pm \gamma_1\gamma_2)$, we can observe that this unitary operator gives the desired action.

$$U_{12}^-\gamma_1(U_{12}^-)^\dagger = \frac{1}{2}(1 - \gamma_1\gamma_2)\gamma_1(1 - \gamma_2\gamma_1) \tag{46}$$
$$= \frac{1}{2}(\gamma_1 - \gamma_1 + \gamma_2 + \gamma_2) = \gamma_2 \tag{47}$$
$$U_{12}^-\gamma_2(U_{12}^-)^\dagger = \frac{1}{2}(1 - \gamma_1\gamma_2)\gamma_2(1 - \gamma_2\gamma_1) \tag{48}$$
$$= \frac{1}{2}(\gamma_2 - \gamma_1 - \gamma_1 - \gamma_2) = -\gamma_1 \tag{49}$$

and similar relations can be checked for U_{12}^+. Unfortunately, if let these act on the physical qubit states:

$$\begin{aligned} U_{12}^-|0\rangle &= U_{12}^- f|1\rangle \qquad (50)\\ &= \frac{1}{\sqrt{2}}(1-\gamma_1\gamma_2)(\gamma_1+i\gamma_2)|1\rangle \\ &= \frac{1}{\sqrt{2}}(f+if)|1\rangle = \frac{1}{\sqrt{2}}(1+i)|0\rangle \\ U_{12}^-|1\rangle &= U_{12}^- f^\dagger|0\rangle \qquad (51)\\ &= \frac{1}{\sqrt{2}}(1-\gamma_1\gamma_2)(\gamma_1-i\gamma_2)|0\rangle \\ &= \frac{1}{\sqrt{2}}(f^\dagger+if^\dagger)|0\rangle = \frac{1}{\sqrt{2}}(1+i)|1\rangle \end{aligned}$$

they just change the phase, meaning the braiding can't change the physical qubit state. Thus, we are forced to create logical qubits, which come from a pair of Kitaev chains, meaning it requires 4 end modes to create a single bit:

$$|0\rangle_L = |00\rangle \qquad (52)$$
$$|1\rangle_L = |11\rangle = f_1 f_2|00\rangle \qquad (53)$$

where the L stands for logical, and the subscript on f indexes the chain. Now observe,

$$\begin{aligned} U_{23}^-|0\rangle_L &= \frac{1}{\sqrt{2}}(1-\gamma_2\gamma_3)|00\rangle \qquad (54)\\ &= \frac{1}{\sqrt{2}}(1-\gamma_2\gamma_3)(\gamma_1+i\gamma_2)(\gamma_3+i\gamma_4)|11\rangle \qquad (55)\\ &= \frac{1}{\sqrt{2}}(|00\rangle - i|11\rangle) = \frac{1}{\sqrt{2}}(|0\rangle_L - i|1\rangle_L) \qquad (56) \end{aligned}$$

and similarly, $U_{23}^-|1\rangle_L = \frac{1}{\sqrt{2}}(|1\rangle_L - i|0\rangle_L)$, $U_{23}^+|0\rangle_L = \frac{1}{\sqrt{2}}(|1\rangle_L + i|0\rangle_L)$, and $U_{23}^+|1\rangle_L = \frac{1}{\sqrt{2}}(|1\rangle_L + i|0\rangle_L)$. From this, more interesting gates can be constructed. In fact, braiding allows the construction of every single qubit gate (up to a constant factor) [23]:

$$H = U_{12}^+ U_{23}^+ U_{12}^+ \qquad (57)$$
$$iX = U_{23}^+ U_{23}^+ \qquad (58)$$
$$-iY = U_{24}^+ U_{24}^+ \qquad (59)$$

where H is Hadamard, X, Y are the associated Pauli matrices. Thus, every single qubit gate can be realized. To perform a 2 qubit gate like CNOT requires braiding 8 particles, which is possible, but notationally ugly. See instead [24]. With these gates, this forms a universal set, which would be totally topologically protected.

3.2 Fibonacci Anyons

Another model to be considered are Fibonacci anyons, which are defined by their fusion rules, or the so called "F-matrix" [25, 26].

$$\tau \times \mathbf{1} \to \tau \tag{60}$$
$$\mathbf{1} \times \tau \to \tau \tag{61}$$
$$\tau \times \tau \to \mathbf{1} \oplus \tau \tag{62}$$
$$\mathbf{1} \times \mathbf{1} \to \mathbf{1} \tag{63}$$

We can map the Rydberg system onto this in a very straightforward manner, by making the association $|r\rangle \leftrightarrow \mathbf{1}, |g\rangle \leftrightarrow \tau$ [27].

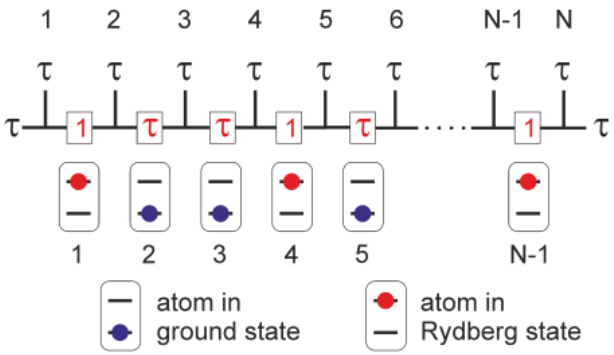

Figure 4: A Fusion chain encoded in Rydberg atoms, image from [27].

Now, a chain of atoms initially prepared in the ground state, and under a driving laser field to create the Rydberg blockade Hamiltonian, can encode a Fibonacci fusion chain in its states. A fusion chain is defined as a collection of anyons that consecutively fuse together [25, 26]. In the Rydberg case, the specific fusion chain is beginning with a single τ, and at each step, fusing with another τ. Each Rydberg atom in the lattice encodes the product of the fusion at each step. This process works because next to a ground state atom can be either a ground or Rydberg - i.e. $|g\rangle \times |g\rangle \to |g\rangle \oplus |r\rangle$, and next to a Rydberg has to be a ground state atom by the blockade effect, i.e. $|r\rangle \times |g\rangle \to |g\rangle$, which is exactly what was required by the Fibonacci fusion rules under the Rydberg mapping. Therefore, any 1D lattice of atoms separated so that only nearest neighbors are being blockaded, and under a continuous driving field resonant with a Rydberg transition, will naturally align with a Fibonacci fusion chain.

Now, consider computation with the Fibonacci anyons. Because they are also non-abelian anyons, just like the Majoranas (they also happen to be self-adjoint), they have a non-abelian braid group, as well. In this way, it is possible for one to demonstrate universality of its gates, just like before, see [25].

In both the Fibonacci and the Kitaev chain, there are distinct advantages to be had from using a neutral atom platform. Because the atoms are held in free space by optical tweezers, braiding becomes particularly trivial, as one simply needs to physically move the particles about each other in real space. Other platforms require complicated mechanisms to move the anyons around [10]. Further, state readout is done simply by physically imaging the atoms, which can be made to be fast, and allows readout of the entire lattice simultaneously if desired. For these reasons, in addition to the wide number of tools for simulating Hamiltonians, neutral atoms are a particularly exciting platform on which to try and realize topologically protected qubits.

References

[1] Feynman, R.P. Simulating physics with computers. Int J Theor Phys 21, 467–488 (1982). https://doi.org/10.1007/BF02650179

[2] Arute, F., Arya, K., Babbush, R. et al. Quantum supremacy using a programmable superconducting processor. Nature 574, 505–510 (2019). https://doi.org/10.1038/s41586-019-1666-5

[3] Blume-Kohout, R., Gamble, J., Nielsen, E. et al. Demonstration of qubit operations below a rigorous fault tolerance threshold with gate set tomography. Nat Commun 8, 14485 (2017). https://doi.org/10.1038/ncomms14485

[4] Wendin, G. "Quantum information processing with superconducting circuits: a review." Reports on Progress in Physics 80.10 (2017): 106001.

[5] Bruzewicz, Colin D., et al. "Trapped-ion quantum computing: Progress and challenges." Applied Physics Reviews 6.2 (2019): 021314.

[6] Levine, Harry, et al. "High-fidelity control and entanglement of rydberg-atom qubits." Physical review letters 121.12 (2018): 123603.

[7] Resch, Salonik, and Ulya R. Karpuzcu. "Quantum computing: an overview across the system stack." arXiv preprint arXiv:1905.07240 (2019).

[8] Kitaev, A. Yu. "Fault-tolerant quantum computation by anyons." Annals of Physics 303.1 (2003): 2-30.

[9] Munkres, James. "Topology James Munkres Second Edition."

[10] Alicea, Jason. "New directions in the pursuit of Majorana fermions in solid state systems." Reports on progress in physics 75.7 (2012): 076501.

[11] Kitaev, A. Yu. "Unpaired Majorana fermions in quantum wires." Physics-Uspekhi 44.10S (2001): 131.

[12] Trebst, Simon, et al. "A short introduction to Fibonacci anyon models." Progress of Theoretical Physics Supplement 176 (2008): 384-407.

[13] Browaeys, Antoine & Barredo, Daniel & Lahaye, Thierry. (2016). "Experimental investigations of the dipolar interactions between single Rydberg atoms." https://arxiv.org/abs/1603.04603

[14] Madjarov, I, et al. "High-Fidelity Control, Detection, and Entanglement of Alkaline-Earth Rydberg Atoms" arXiv:2001.04455 (2020)

[15] Daniel A. Steck, "Rubidium 87 D Line Data," available online at http://steck.us/alkalidata (revision 2.2.1, 21 November 2019).

[16] Schlosser, Nicolas, Georges Reymond, and Philippe Grangier. "Collisional blockade in microscopic optical dipole traps." Physical review letters 89.2 (2002): 023005.

[17] Urban, E., Johnson, T., Henage, T. et al. "Observation of Rydberg blockade between two atoms." Nature Phys 5, 110–114 (2009). https://doi-org.proxy.uchicago.edu/10.1038/nphys1178

[18] Browaeys, Antoine. "Realizing quantum Ising models in tunable two-dimensional arrays of single Rydberg atoms." APS Meeting Abstracts. 2019.

[19] Barredo, Daniel, et al. "Coherent excitation transfer in a spin chain of three Rydberg atoms." Physical review letters 114.11 (2015): 113002.

[20] Wigner, Eugene P., and Pascual Jordan. "Über das Paulische Äquivalenzverbot." Z. Phys 47 (1928): 631.

[21] Kitaev, Alexei, and Chris Laumann. "Topological phases and quantum computation." Exact methods in low-dimensional statistical physics and quantum computing," Lecture Notes of the Les Houches Summer School 89 (2009): 101-125.

[22] Labuhn, H., Barredo, D., Ravets, S., de Léséleuc, S., Macrì, T., Lahaye, T., & Browaeys, A. (2015). Realizing quantum Ising models in tunable two-dimensional arrays of single Rydberg atoms. arXiv preprint arXiv:1509.04543.

[23] Ostnell, Sebastian. "Quantum Gates Using Majorana Modes in Nanowires." 2019. University of Gothenberg, Master's Thesis.

[24] Litinski, Daniel, and Felix von Oppen. "Braiding by Majorana tracking and long-range CNOT gates with color codes." Physical Review B 96.20 (2017): 205413.

[25] Field, Bernard, and Tapio Simula. "Introduction to topological quantum computation with non-Abelian anyons." Quantum Science and Technology 3.4 (2018): 045004.

[26] Trebst, Simon, et al. "A short introduction to Fibonacci anyon models." Progress of Theoretical Physics Supplement 176 (2008): 384-407.

[27] Lesanovsky, Igor, and Hosho Katsura. "Interacting Fibonacci anyons in a Rydberg gas." Physical Review A 86.4 (2012): 041601.